

LUMINESCENT SOLAR NOISE BARRIER – LARGE SCALE TESTING AND MODELING

L.H. Slooff¹, S. Verkuilen², M.M. de Jong³, M.N. van den Donker³, M. Kanellis⁴, M.G. Debije⁵

¹ECN Solar Energy, P.O. Box 1, 1755 ZG Petten, The Netherlands

²Heijmans Wegen B.V., Graafsebaan 67, P.O. Box 5248 JT Rosmalen, The Netherlands

³SEAC, High Tech Campus 21, 5656AE Eindhoven, The Netherlands

⁴Smart Energy Buildings & Cities, Eindhoven University of Technology, 5600 MB Eindhoven, The Netherlands

⁵Chemical Engineering & Chemistry, Eindhoven University of Technology, P.O. Box 513, 5600 MB Eindhoven, The Netherlands

Phone: +31 88 515 4314, Fax: +31 88 515 8214, E-mail: slooff@ecn.nl

ABSTRACT: Two modular noise barrier test setups containing photovoltaic modules have been installed in the Netherlands, one in a North/South orientation, and the other in East/West orientation. Both setups contain one set of mono-facial c-Si panels, one set of bi-facial c-Si panels and two luminescent solar concentrator (LSC) panels, one red and one orange/yellow. The performance of all panels is monitored along with the irradiation and temperature data. Here we will focus on the performance of the two LSC panels and present the results of a ray-tracing model that mimics the situation at the demo site.

Keywords: Luminescent Solar Concentrator, Modelling, Field Test, Noise Barrier

1 INTRODUCTION

Noise barriers offer the enormous potential of using the otherwise unproductive area along highways and railways for energy production. There are a few demonstration installations using traditional silicon-based solar panels [1,2,3,4]. Luminescent solar concentrators (LSCs) could play a role in initiating the large scale implementation of energy producing noise barriers. The different colors potentially offer more variety in the design of the barriers compared to traditional PV panels. Furthermore, LSCs are (semi)-transparent, which is generally more appreciated by the community and in some cases even a requirement for noise barriers. Although there have been some larger scale applications of LSCs, not much is known about their annual performance.[5,6,7] This study provides experimental and theoretical data on a large scale test setup which enables performance prediction of an LSC noise barrier with different orientations, sizes and colors. The results form the basis of a study to determine if a solid business case can be made for noise barriers based on LSCs.

2 LUMINESCENT SOLAR CONCENTRATORS

A luminescent solar concentrator normally consists of a polymer plate that contains luminescent species like organic dyes or inorganic quantum dots. Solar light is incident on the plate and is absorbed by the luminescent particle and subsequently emitted. See Fig. 1

The light is emitted such that a fraction of the light will be trapped inside the plate by total internal reflection. This trapped light will travel through the light guide until it reaches one of the side edges. PV cells are connected to the sides to convert the emission light into electricity. This concept was first introduced in the mid 70's. [8,9,10,11].

The LSC has an important advantage over geometric concentrators in that both direct and diffuse sunlight is collected, making solar tracking unnecessary [12]. This makes them especially interesting for building integration applications.

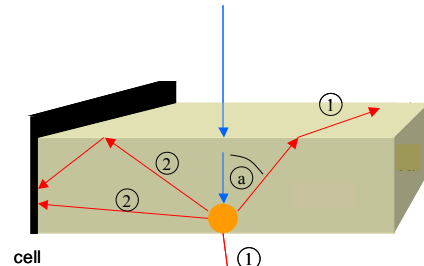


Figure 1: Schematic 3D view of a luminescent concentrator. Light is incident from the top. The light is absorbed by a luminescent particle. The luminescence from the particle is emitted. A fraction of the emission falls within the escape cone (determined by the angle (a)) and is lost from the LSC through the surfaces (1). The remaining fraction of the luminescence is guided to the Si cell by total internal reflection (2)

3 TEST INSTALLATION

A commercial modular noise barrier forms the basis of the test installation. Instead of the standard noise barrier glass or plastic, the setup contains 4 different types of panels: one set of glass/glass mono-facial c-Si panels, one set of glass/glass bi-facial c-Si panels and two luminescent solar concentrator (LSC) panels, one red and one orange/yellow (see Fig. 2). The site consists of two modular noise barriers, one facing North/South and one facing East/West. The barriers are tilted 15° towards the North and East, respectively. The individual panels are 1 m high and 5 meters long. A photograph of the experimental site is shown in Fig. 3. In this paper we will focus on the LSC part of the noise barrier.



Figure 2: Artist impression of the modular noise barrier.



Figure 3: Photograph depicting the test setup of the two modular noise barriers

4 APPROACH

4.1 The ray tracing model

A ray-tracing model was used to simulate the performance of the test setup. In the model a ray represents light of a specific wavelength travelling in a given direction. A ray that is incident on an air- LSC interface can proceed in two ways; it can either be reflected, or transmitted. In ray-tracing, random numbers are generated and used to determine the fate of the ray in such a situation. Consider for example a reflection at an interface with a reflection coefficient of 30%. A random number r is drawn from a uniform distribution in the interval $[0,1]$. If $r < 0.3$ the ray is reflected, if $r \geq 0.3$ the ray is transmitted. This ray-tracing model has been used previously for modelling lab-scale LSCs and demonstrated accurate predictions when compared to experimental results for LSCs of various sizes, dye content and photovoltaic cell attachments.[13,14,15] Input for the model are the dye absorption and emission characteristics, concentration, luminescence quantum yield and the polymer optical constants. Emission of the dyes is assumed to be in random direction. Only direct illumination of the plates is taken into account. The test set-up contains series connected c-Si cells at various positions along the top and bottom side of the LSC plates. For the PV cells, typical internal quantum efficiency data are used and other parameters were taken from fits to measured I-V data. The basics of the model were first compared to reflection and transmission measurements of the LSC plate material. When transmission and reflection are measured using an integrating sphere, light emitted by the dye will also be detected. An estimate of the dye the luminescent quantum yield (LQY) was obtained by fitting the LQY in the model to match the dye emission part in the experimental reflection and transmission measurements. Subsequently the model was compared with the actual demonstration panel results using the derived LQY values for the dyes. Finally, improvements in LSC noise barrier design are considered to optimize the performance.

4.2 Calculation results

Comparison of the model calculation with data from the test site for a sunny day on May 24, 2015, shows an excellent correlation. Figure 4 shows the normalized power and calculated results for one of the c-Si cell strips

at the top of the south-facing red plate. Figure 5 depicts similar results for c-Si cells at the bottom and Fig. 6 the results for the orange plate.

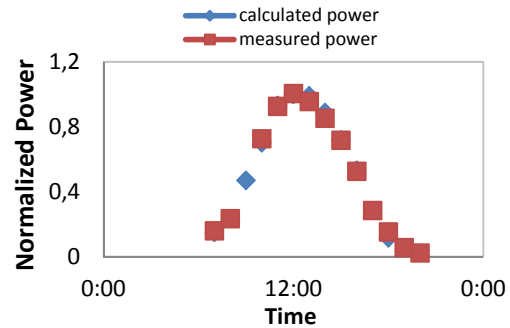


Figure 4: Calculated (blue, diamond) and measured (red, square) power from c-Si cells at the top of the red South-facing LSC panel

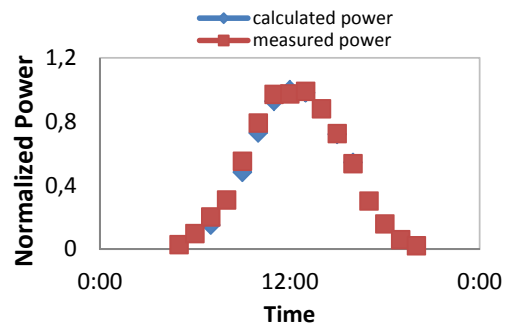


Figure 5: Calculated (blue, diamond) and measured (red, square) power from c-Si cells at the bottom of the red South-facing LSC panel

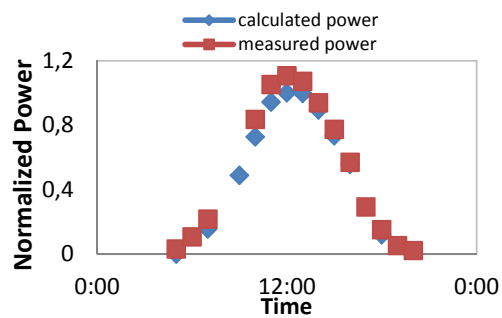


Figure 6: Calculated (blue, diamond) and measured (red, square) power from c-Si cells at the bottom of the orange South-facing LSC panel

In the model there were two fit parameters, the temperature coefficient of the V_{oc} and the dark saturation current I_0 . For the c-Si cells a temperature coefficient of -3.8 mV/K was found and an I_0 of 1.1×10^{-11} - 1.3×10^{-11} A. As for the overall power, the V_{oc} and I_{sc} matched nicely with the measured data, as can be seen for the V_{oc} in Fig. 7 and 8.

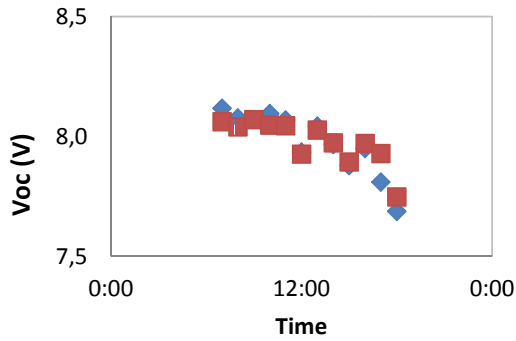


Figure 7: Measured (red, square) and calculated (blue, diamond) V_{oc} of the top c-Si cells on the South-facing red panel

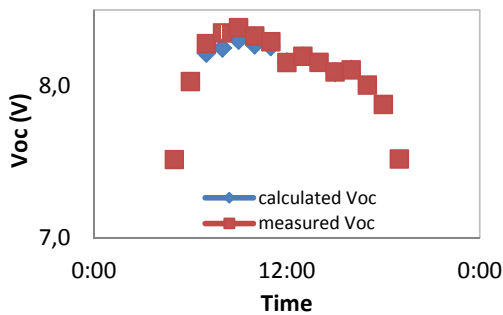


Figure 8: Measured (red, square) and calculated (blue, diamond) V_{oc} of the top c-Si cells on the South-facing orange panel

The observed changes in V_{oc} over the day are due to changes in both the temperature and irradiation conditions.

The results for the East/West oriented panels show some interesting results. Of course, the trend over the day is different as the sun rises in the East, thereby first illuminating the panel from the back side. Near noon it is illuminating the panel from overhead and in the afternoon from the front side. As the supporting aluminum structure at the top extends at the back, this results in shadowing of the rear side as the sun moves to the front. This only affects the cell strips at the top side of the East/West oriented panels, see Fig. 9.



Figure 9: Schematic of the East/West oriented LSC in the morning looking from the East. The supporting construction induces a shadow (grey bar) along the top of the rear side, thereby affecting the output of the top cells

The effect of this shadowing can be seen in Fig. 10-11. In the morning, the modelled data predict a higher

output power than was measured, whereas in the afternoon the model matches the measured results. The difference between the model and the measurement in the morning give an indication of the power that is lost due to self-shadowing by the supporting construction.

These observations makes it clear that for the East/West orientation it is especially important to minimize the self-shadowing of the supporting construction, although complete elimination of shadowing will not be possible. Calculations can be done to estimate the effect of the shadowing on the output of the cells to determine an optimum interconnection scheme for the cells and thereby minimizing the effect of the shadowing.

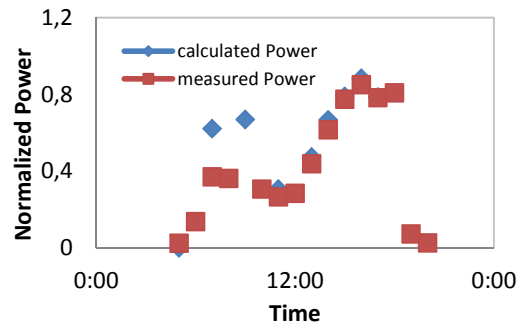


Figure 10: Calculated and measured power from c-Si cells attached to the top left of the West-facing red LSC panel

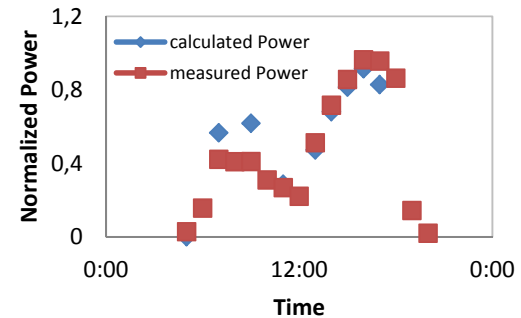


Figure 11: Calculated and measured power from c-Si cells at the top right of the red West-facing LSC panel. The effect of the shadow from the supporting frame on the output is clearly seen around 10:30

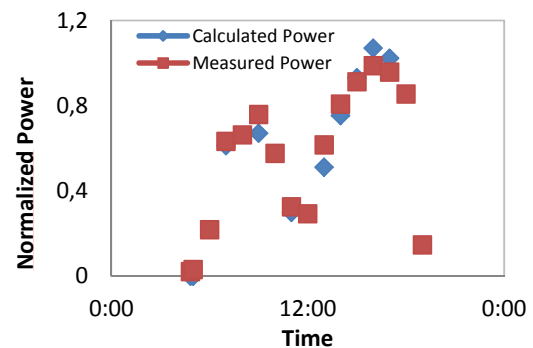


Figure 12: Calculated and measured power from c-Si cells at the bottom of the red West-facing LSC panel

Figure 12 shows the results for one of the bottom mounted c-Si cells. Clearly these cells do not suffer from self-shading by the supporting frame.

4.3 Optimization

Now that the model has been verified with the experimental data, it can be used to perform a parameter study to see if the performance can be optimized. As a start, the effect of varying the panel height and panel thickness has been tested. The result is shown in Fig. 13 where the panel height was varied from 0.3 to 1.0 m and the panel thickness from 12 to 20 mm. Reducing the panel height increases the response, as the shorter travel distance of the emission light results in less light being lost by scattering and (re-) absorption on its way to the cells at the side. An increase in thickness results in an increase in the performance of the panel. Due to the greater thickness, the light encounters less reflections at the front and rear side. As each reflection gives a chance for the light to escape the plate, less reflections will result in a higher performance. In addition, on average the dye molecules are more distant from one another, increasing the path length of emission light between encounters, reducing re-absorption and the associated losses.

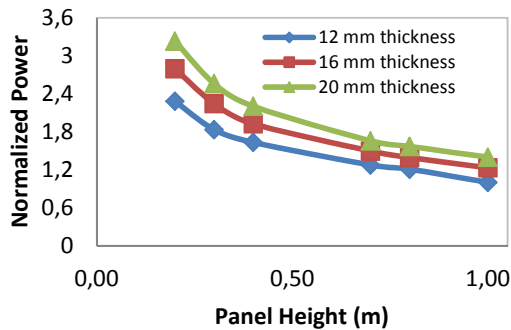


Figure 13: Normalized power output from c-Si cells at the bottom of the red West-facing LSC panel as a function of increased panel thickness and reduced panel height

5 CONCLUSIONS

Experimental results from a large scale luminescent solar concentrator (LSC) noise barrier test setup have been compared with the results from a ray-tracing model for a sunny day. The results show a good comparison between the model and the actual data for both the North/South and East/West barrier orientations. The data from the actual test site show the importance of reducing the shadowing losses caused by the supporting frame. The model can also be used to estimate the performance distribution along the sides of the LSC, thereby proving input for optimization of the electrical interconnection of the cells. Calculations show that the performance of the LSC noise barrier can be improved by increasing the thickness of the panels and by reducing the height. The latter will be at the expense of an increased number of cells. Cost calculations must be performed to determine if the improved performance outweighs the additional cell costs. Further work will focus on the use of the model for annual yield prediction of LSC based noise barriers.

6 ACKNOWLEDGMENTS

This work has been supported by the Dutch Government through the TKI ZEGO program. The authors would also like to acknowledge the other project partners: van Campen Industries BV, and Airbus Defence and Space for their support and the city of Den Bosch for making the test location available.

- [1] Noise reduction B31 Germany
http://pvdatabase.org/projects_view_details.php?ID=376
- [2] Arras Highway21 Noise Barrier France
http://pvdatabase.org/projects_view_details.php?ID=91
- [3] PV noise barrier A9 The Netherlands
http://pvdatabase.org/projects_view_details.php?ID=390
- [4] PV noise barrier A27 The Netherlands,
http://pvdatabase.org/projects_view_details.php?ID=74
- [5] P. Bernardoni, R. Zarcone, M. Tonezzer, D. Vincenzi, M. Brocato, G. Calabrese, V. Guidi, S. Baricordi, Proceedings 31st EU-PVSEC (2015) 29034
- [6] P. Bernardoni, M. Tonezzer, D. Vincenzi, V. Guidi, S. Baricordi, G. Calabrese, Proceedings 31st EU-PVSEC (2015) 2639
- [7] P. Bernardoni, M. Tonezzer, D. Vincenzi, S. Baricordi, G. Calabrese, V. Guidi, Proceedings 31st EU-PVSEC (2015) 1429
- [8] W.H.Weber, J.Lambe, Appl. Opt. 15 (1976) 2299
- [9] C. F.Rapp, Norman L.Boling, Proceedings 13th IEEE Photovoltaic Specialists Conference (1978) 690
- [10] A. Goetzberger and W. Greubel, Appl. Phys. 14 (1977) 123
- [11] M.G. Debije, P.P.C. Verbunt, Adv. En. Mat. 2 (2012) 12
- [12] M.G. Debije, V. A. Rajkumar, Solar Energy, Volume 122 (2015) 334
- [13] A.R. Burgers, L.H. Slooff, R. Kinderman, J.A.M. van Roosmalen, Proceedings of the 20th EUPVSEC (2005) 394
- [14] A., R. Burgers, L.H. Slooff, A. Büchtemann, J.A.M. van Roosmalen, Proceedings of the IEEE 4th WCPEC (2006) 198
- [15] L.H. Slooff, R. Kinderman, A.R. Burgers, A. Büchtemann, R. Danz, T.B. Meyer, A.J. Chatten, D. Farrell, K.W.J. Barnham, J.A.M. van Roosmalen, SPIE Proceedings Vol 6197 (2006) 61970k1